

Dynamic analysis of a multi-span simply supported prestressed concrete bridge with restrainers and seismic isolation devices

Ouanani M ^{1,3*}, Sandjak K^{2,3}, Tiliouine B³

1 Université de Djelfa, Faculté des Sciences et de la Technologie, Djelfa, ALGERIA.

2 Département de Génie Civil, Faculté des Sciences de l'Ingénieur, Université M'Hamed Bougara, 35000, Boumerdes, ALGERIA.

3 Ecole Nationale Polytechnique, Département de Génie Civil, Laboratoire de Génie Sismique et de Dynamique des Structures, 10 Avenue des Frères Oudek, Hassen Badi, BP. 182, 16200, El Harrach, Alger, Algérie Dynamics, Alger, ALGERIA

* Corresponding Author: mouloud.ouanani@g.enp.edu.dz, m.ouanani@univ-djelfa.dz

Received: 16-06-2020

Accepted: 24-08-2020

Abstract. The Nonlinear F.E. code Structural Analysis Program (SAP) in which the primary nonlinear characteristics of bearings, impact elements and steel restrainer cables considered herein in order to investigate the dynamic analysis of a multi-span simply supported MSSS prestressed concrete bridge, equipped with steel restrainer cables and Lead Rubber Bearings LRB devices including Soil Structure Interaction (SSI) effects. A MSSS bridge with restrainer cables and lead rubber bearings at the two abutments and intermediate bents located in North Algeria is selected according to RPOA for seismic design category 1 is considered in this study. A detailed 3D nonlinear analytical model of study bridge subjected to three components identical seismic excitation including pounding elements, restrainer cables and bearing devices at expansion joints is developed. The nonlinear characteristics of these boundary elements are represented by bilinear hysteretic models. Under strong seismic excitations, the large longitudinal displacements result the collision between bridge decks or even unseating of these decks at expansion joints of MSSS bridge. Finally, the study reveals among others that in order to prevent deck unseating resulting from restrainer failures and subsequent bridge collapse, particular attention should also be given to proper design of nonlinear characteristics of restrainers and bearing devices.

Key words: Nonlinear F.E., Soil structure interaction, pounding elements, restrainer cables, lead rubber bearings

1. Introduction

The multi-span simply supported MSSS prestressed concrete bridges are frequently used in highway bridges representing an essential component of transportation networks. This category of bridges presents various advantages such as, fast construction, convenient manufacture and installation and their adjacent bridge decks are connected at expansion joints in order to accommodate temperature and deformations induced by shrinking and creep of prestressed concrete. Unfortunately, the expansion joints between adjacent decks or between deck and abutment become vulnerable components under severe ground motions, because of the superstructure pounding which may induce the local failure of the deck itself and unseating damage.

However, the MSSS highway bridge damages due to pounding impact at the expansion joints of girders and abutments and unseating have been particularly observed in several seismic events, (e.g. Wenchuan earthquake (Hung et al., 2008), Boumerdes earthquake (AFPS, 2003), Chi-Chi earthquake (Uzarski and Arnold, 1999), Kobe earthquake (Chouw, 1995) and Northridge earthquake (Todd et al., 1994)). In particular, the Chi-Chi earthquake (1999) in Taiwan revealed hammering at the expansion joints in some bridges which resulted in damage to shear keys, bearings and anchor bolts (Uzarski and Arnold, 2001). Based on these observations, pounding

can cause crushing and spalling of concrete at the impact locations, result in damage to column bents, abutments, shear keys, bearing pads and restrainers, and possibly contribute to the collapse of deck spans.

Many previous works have been conducted to investigate the fragility of highway bridges under uniform ground motions (Shinozuka et al., 2003; Desroche and Muthamar, 2004; Hong et al., 2019) and non uniform ground motions (Yang et al., 2018), they corroborated that the multi-span simply supported MSSS prestressed concrete bridges are most vulnerable to pounding damage due to the discontinuity in the superstructure at multi-column bents. In particular, Hong et al. (2019) investigated the effect of the nonlinear impact on the longitudinal response of multi-span simply supported bridges under strong earthquakes and they concluded that the collision parameters affect the responses of the multi-span simply supported beam bridge subjected to ground motions. Further researches by Bi et al. (2013) and Yang et al. (2018) have also studied extensively the impact of spatially varying ground motions on the seismic response of bridges when pounding was either considered or not considered.

In addition to above practical justifications, the damage data of bridges have also illustrated that the bridge components structural performance may be very sensitive to 3D components of ground motions (Tiliouine and Ouanani, 2012) and foundation soil flexibility including abutment-backfill soil (Ouanani and Tiliouine, 2017).

This paper presents some results from an exhaustive investigation carried out on the dynamic analysis of a multi-span simply supported MSSS prestressed concrete bridge equipped with restrainers and seismic isolation devices at expansion joints and abutments including Soil Structure Interaction (SSI) effects. In this context, The nonlinear time history analyses using detailed 3D Finite Element Model FEM of a MSSS bridge located in North Algeria are performed to assess the performance of the steel restrainer cables and Lead Rubber Bearing devices LRB under the 3D components of severe seismic excitation. Nonlinear characteristics of the impact and restrainer elements at expansion joints and bearing devices at the seat-abutments and intermediate bents of study bridge are represented by nonlinear hysteretic models. These nonlinear properties are considered in the dynamic analysis of a multi-span simply supported concrete bridge. These considered nonlinearities include the width of expansion joint, the impact stiffness of colliding spans and the longitudinal stiffness of the bearing device in the seismic analysis in order to predict or to avoid the collision damages in bridge structures. In order to include the SSI effects, the effective stiffness, foundation soil damping at the base of the spread footings have been evaluated using procedure guidelines (FEMA, 2000).

2. Description and 3-D nonlinear analytical model of MSSS prestressed concrete bridge

2.1. Description of MSSS prestressed concrete bridge

Fig. 1 shows details of typical MSSS pre-stressed concrete girder bridge located on the East-West highway joining the Bouira City in Eastern Algeria. The bridge considered in this study is straight with slope of 4.60% and consists of a three discontinued decks reinforced concrete of 13.1 m wide and equal length of 35.85m (Figures. 1(a), 1(b)) and supported by seven prestressed concrete T girders (Figure 1(c)).

The bridge with an overall length of 107.77m is supported on multi-column bents of equal height of 19.3m and two seat-type abutments. Each column has a circular cross-section with 1.8 m diameter (Figure 1(d)).

The bridge consists of four expansion joints in steel of type Wd110, located on the two Multi-column bents and the two abutments. Each pre-stressed concrete T-shaped girder is supported at abutments and bents by the Lead Rubber Bearing device LRB.

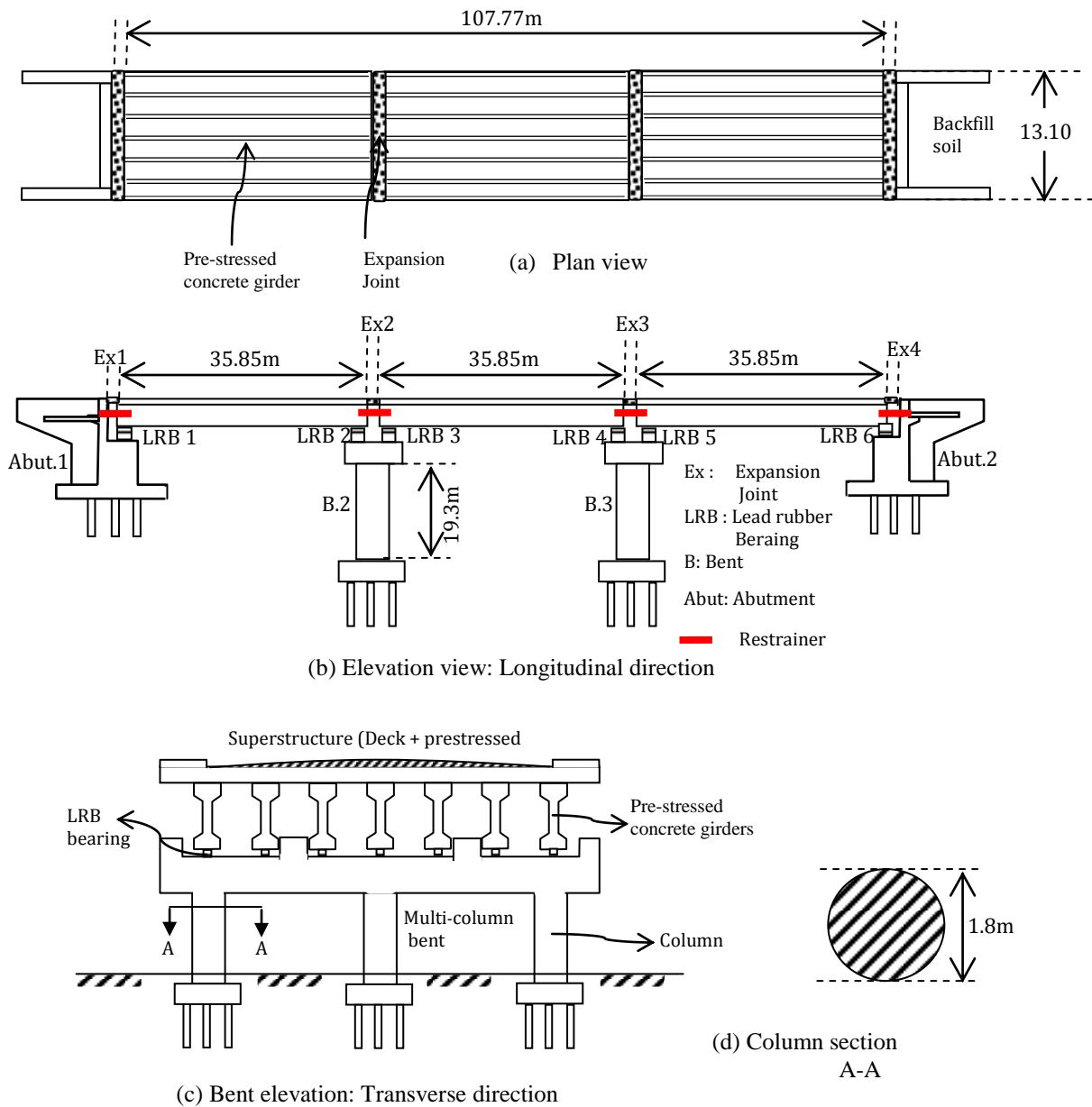


Fig 1. General description of MSSS prestressed concrete bridge.

2.2. 3D nonlinear analytical modeling of MSSS prestressed concrete bridge

The MSSS bridge with steel restrainer cables and lead rubber bearings at two abutments and intermediate bents considered in this study is analytically modeled as a lumped mass system. Thus, a 3D nonlinear analytical model of a bridge is developed using the Nonlinear F.E. code (CSI Bridge, 2015). The superstructure and multi-columns bents of bridge are modelled as elastic-beam elements, while bridge additional connecting components such as the expansion joints that represent pounding elements are modelled by linear spring elements, while the lead rubber bearings and restrainer cables are modelled by nonlinear spring elements accounting the energy dissipation under strong motion.

2.2.1 Analytical modeling of restrainer cables elements

Restrainer cable elements are devices which permit the limitation of the deck longitudinal displacement and relative hinge openings in order to prevent unseating of bridge spans, or as fail-safe mechanisms to support bridge decks in case of unseating. They are often employed in bridges with insufficient seat widths and placed at the hinge locations at the deck abutment and deck-bent cap interfaces in the (MSSS) bridge considered herein. In general, the restrainer cables are employed in order to avoid unseating of the superstructure at the expansion joints. The restrainers alter the behavior of adjacent spans by transferring forces as the span opening exceeds the slack in the cable. Three types of restrainers are used in order to assess the seismic performance of a MSSS bridge: the steel restrainer cables (SRC), the Shape Memory Alloy (SMA) bars in tension (SMA-T), and the SMA bars in bending (SMA-B) (Desroches and Delemont, 2002; Tazarv and Alam, 2018).

For the considered bridge, the SRC devices connecting the adjacent spans at the expansion joints as shown in Fig. 1(b) are used herein in order to investigate the dynamic analysis of a multi-span simply supported MSSS.

2.2.2 Analytical modeling of pounding elements

Two analytical methods are available for simulating the highly nonlinear behavior of pounding at the interface span-abutment and span-span; the stereo mechanical method and that of the contact element. The latter is activated when the collision occurs between decks/abutments and deck/deck of the bridge. The spring stiffness of pounding elements is fixed proportionally to the axial stiffness of the neighboring structural segments, sometimes in combination with a damper (Kawashima and Shoji, 2000; Hong et al., 2019), the spring stiffness, K_{gap} is expressed as:

$$K_{gap} = \gamma \frac{EA}{L} \quad (1)$$

where EA represents the axial stiffness of the cross-section of the superstructure, L is the length of the superstructure's element, and γ is the ratio of impact spring stiffness to that of the superstructure.

The gap provided at the expansion joint is 11 cm and adjacent spans collision develop compressive forces when the relative displacement exhausts this gap width. It is modelled by the Kelvin model with stiffness $K_{gap} = 45.87 \times 10^6$ KN/m. The compressive forces (f_p) for this model are expressed as follows (Desroche and Muthamar, 2004; Hong et al., 2019):

$$\begin{aligned} \text{If } (d - gap) > 0, f_p &= K_g \times (d - gap) + C \times (\dot{d}) \\ \text{Otherwise, } f_p &= 0 \end{aligned} \quad (2)$$

d is given as.

$$\begin{aligned} d &= u_i - u_j; \\ \dot{d} &= \dot{u}_i - \dot{u}_j \end{aligned} \quad (3)$$

where u_i and u_j are the displacements of nodes i and j respectively, gap is separation between these nodes, \dot{u}_i and \dot{u}_j are the velocities of nodes i and j respectively.

The dashpot constant of the Kelvin model is calculated using these formulas

$$C = 2\xi \times \sqrt{\left(K_p \frac{m_1 m_2}{m_1 + m_2} \right)} \quad (4)$$

$$\xi = -\frac{\ln(e)}{\sqrt{(\pi^2 + (\ln(e))^2)}} \tag{5}$$

where m_1 and m_2 are the masses of the two impacting bodies, the constant (e) is the coefficient of restitution, for which the value is 1 for completely elastic impact and 0 for completely plastic impact (e.g. Anagnostopoulos and Spiliopoulos, 1992).

2.2.3 Analytical modeling of LR Bearing devices

Bridges seismic isolation with Lead Rubber Bearings (LRBs) devices is an effective technique to passively reduce the seismic responses of the bridge. The LRB devices have a nonlinear behavior which may be idealized by a hysteretic bilinear model (see Figure 2).

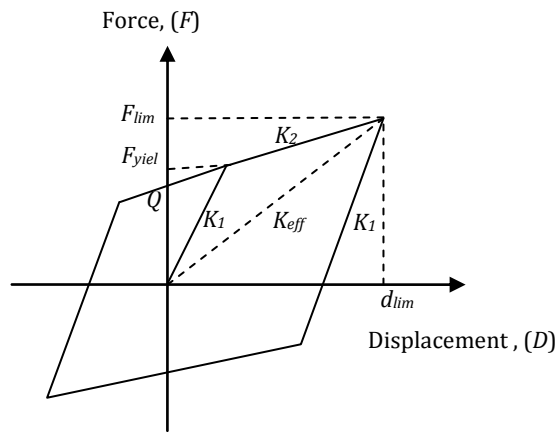


Fig 2. Characteristic curve of the LRB system: hysteretic bilinear model.

The principal parameters that characterize the LRB analytical model are the elastic stiffness K_1 , corresponding to combined stiffness of the rubber bearing and the lead core, the stiffness of the rubber K_2 , and the yield force of the lead core F_{yield} .

The characteristic strength, Q can be accurately estimated as being equal to the yield force of the lead core. F_{lim} and d_{lim} are respectively maximum force and maximum bearing displacement, K_{eff} is effective stiffness of the LRB.

As a rule of thumb for lead-rubber isolators K_1 is taken as $10K_2$, (FEMA, 2000; Xu Chena and Chunxiang, 2020).

The Table 1 reports the parameter values adopted in this study of the LRB analytical model in the longitudinal and lateral directions for a design displacement equal to 0.08m.

Table 1. Parameters of the bilinear model for LRB

Direction	K_1 (KN/m)	K_2 (KN/m)	K_{eff} (KN/m)	Q (KN)	F_{yield} (KN)	C
Longitudinal and lateral	1634	163.4	357.65	15.50		85.33

2.2.4 Analytical modeling of dynamic soil structure interaction

The complex dynamic impedance Z of the soil foundation is expressed as (e.g. Gazetas, 1991; Wolf, 1997):

$$Z = K + i\omega C \tag{6}$$

where K and ωC are real and imaginary parts of the dynamic impedance complex function, the damping coefficient C expresses the radiation that arise from waves emanating away from the foundation soil. Table 2 summarizes the relationships expressing the static stiffnesses of springs and damping coefficients corresponding to the six degrees of freedom at the base of the supports of bridge piers. (e.g. Ouanani and Tiliouine, 2015; Gazetas, 1991).

Table 2. Dynamic impedance complex function of foundation soil

Degrees of freedom	Stiffness of foundation soil	Damping coefficient
Longitudinal direction	$K_x = \frac{8G}{2-\nu} R_x$	$C_x = \frac{4.6G}{(2-\nu)V_s'} R_x^2$
Lateral direction direction	$K_y = \frac{8G}{2-\nu} R_y$	$C_y = \frac{4.6G}{(2-\nu)V_s'} R_y^2$
Vertical direction	$K_z = \frac{4G}{1-\nu} R_z$	$C_z = \frac{3G}{(1-\nu)V_s'} R_z^2$
Rocking about the longitudinal, X-axis	$K_{\theta_x} = \frac{8G}{3(1-\nu)} R_{\theta_x}^3$	$C_{\theta_x} = \frac{0.4G}{(1-\nu)V_s'} R_{\theta_x}^4$
Rocking about the lateral, Y-axis	$K_{\theta_y} = \frac{8G}{3(1-\nu)} R_{\theta_y}^3$	$C_{\theta_y} = \frac{0.4G}{(1-\nu)V_s'} R_{\theta_y}^4$
Torque	$K_{\theta_z} = \frac{16G}{3} R_{\theta_z}^3$	$C_{\theta_z} = \frac{0.8G}{V_s'} R_{\theta_z}^4$

In Table 2, R_x , R_y , R_z , R_{θ_x} , R_{θ_y} and R_{θ_z} are equivalent radii for a rectangular foundation with dimensions L and B (L : long side dimension; B : short side dimension) (e.g. Fema 273, 1997; Gazetas, 1991; Wolf, 1997; Yohchia, 1997).

ν represents the Poisson's coefficient, whereas G and V_s' designate the effective shear modulus and the effective shear wave velocity consistent with soil type and PGA design value.

The 2D-FE nonlinear analytical model in the longitudinal direction of MSSS bridge modelled as lumped masses well as its connection components are detailed in Figure 3.

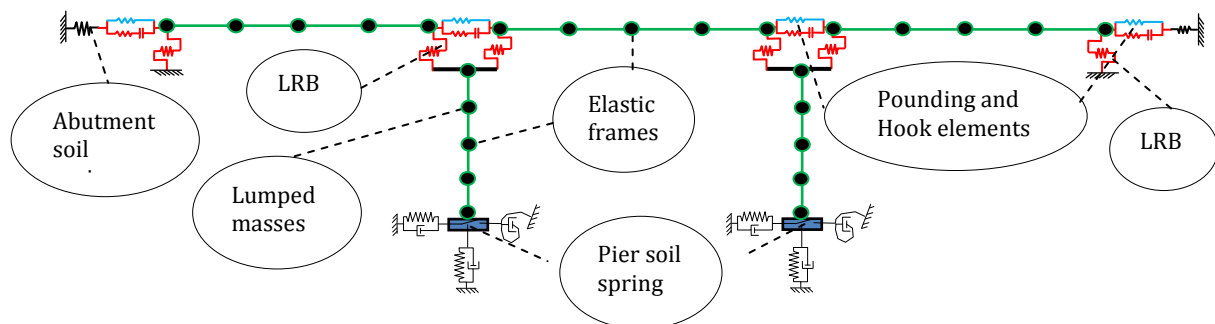


Fig 3. Detail's 2D-FE non linear analytical model in the longitudinal direction of the MSSS bridge and its Components

3. Modal Analysis of a MSSS prestressed concrete bridge- foundation soil system

For free vibration response analysis of a MSSS prestressed concrete bridge-foundation soil systems, the soil structure Interaction is essentially controlled by foundation soil flexibility which in turn is dependent on properties of foundation soil.

In this study, the soil corresponding to the actual condition site construction for the considered bridge is soil type S_2 (firm site) in accordance with RPOA (2008); the weight density $\gamma = 21 \text{ kN/m}^3$; Poisson's ratio $\nu = 0.40$ and initial shear wave velocity $V_s = 400 \text{ m/s}$.

Moreover, the equivalent stiffness and damping coefficients of foundation soil are determined under a simulated accelerogram with PGA equal to 0.275g. The PGA consistent reduction factors for the effective shear modulus G/G_o and the effective shear wave velocity V_s'/V_s are determined using a computer program (SHAKE) for earthquake response analysis of horizontally layered sites Schnabel et al. (1976).

The associated values of coefficients of stiffness and viscous damping foundation soil have been evaluated for soil type S_2 (firm site) with $G/G_o = 0.55$ and $V_s'/V_s = 0.55$.

Table 3. Effective stiffness and effective damping constants of foundation soil.

Rectangular spraed footings			Translational stiffness (KN/m)			Rotational stiffness (KN. m/rd)		
L(m)	B(m)	e(m)	K_x3	K_y2	K_z1	$K_{\theta x}3$	$K_{\theta y}2$	$K_{\theta z}1$
13.2	6.4	1.8	9277264	9055319	9717088	299229684	101021483	259074216
			Translational damping (KN.s/m)			damping rotationnel (KN.m.s/rd)		
			C_x	C_y	C_z	$C_{\theta x}$	$C_{\theta y}$	$C_{\theta z}$
			63027	63027	109612	848832	199542	629024

In this study, numerical techniques (e.g. Wilson, 2002; Chopra, 2011) have been performed in order to identify the dynamic characteristics of the MSSS prestressed concrete bridge.

Table 4 lists the first eleven modal periods and the modal participation factors as well as the corresponding mode types denoted herein by L for lateral, Lg for longitudinal, V for vertical directions and T for torsional vibrations for the coupled bridge structure-foundation soil system.

In addition, the first 3-D modal characteristics of lateral, vertical, longitudinal and torsional vibrations of both symmetrical (S) and unsymmetrical (AS) higher modes of the bridge have been identified. A 3-D graphical representation of the corresponding mode shapes is presented in Figure 4.

Table 4. Modal periods and participation factors vibration modes

Modal orders	Period (sec.)	Participation factors(%)				Mode types
		X-X	Y-Y	Z-Z	R-X	
1	3,445	64,8	0	0	0	First-order Symmetric (S) <u>Longitudinal vibration (Lg)</u>
2	3,398	0	0	0	0	First Anti symmetric (AS) <u>Longitudinal vibration (Lg)</u>
3	3,373	6,7	0	0	0	Second-order Symmetric (S) <u>Longitudinal vibration (Lg)</u>
4	3,184	0	57,2	0	0,1	First-order Symmetric (S) Lateral vibration (L)
5	2,518	0	0	0	0	First-order Antisymmetric (AS) Lateral vibration (L)
6	0,504	0	0	56,4	0	First-order Symmetric (S) Vertical vibration (V)
7	0,502	0	0	0	0	First-order Antisymmetric (AS) Vertical vibration (V)
8	0,500	0	0	0,1	0	Second-order Symmetric (S) Vertical vibration (V)
9	0,476	0	10,1	0	0,1	Coupling modes of L and T vibrations
10	0,473	0	0	0	0	First-order Antisymmetric (S) Torsional vibration (T)
11	0,468	0	0,8	0	3,2	First-order Symmetric (AS) Torsional vibration (T)

From Table 4, it is clearly observed that the first three modes of vibration are longitudinal, which leads to a dynamic analysis in the longitudinal direction (i.e. in the most critical direction) of a multi-span simply supported MSSS prestressed concrete bridge equipped with restrainers and seismic isolation devices at expansion joints and abutments including Soil Structure Interaction (SSI) effects.

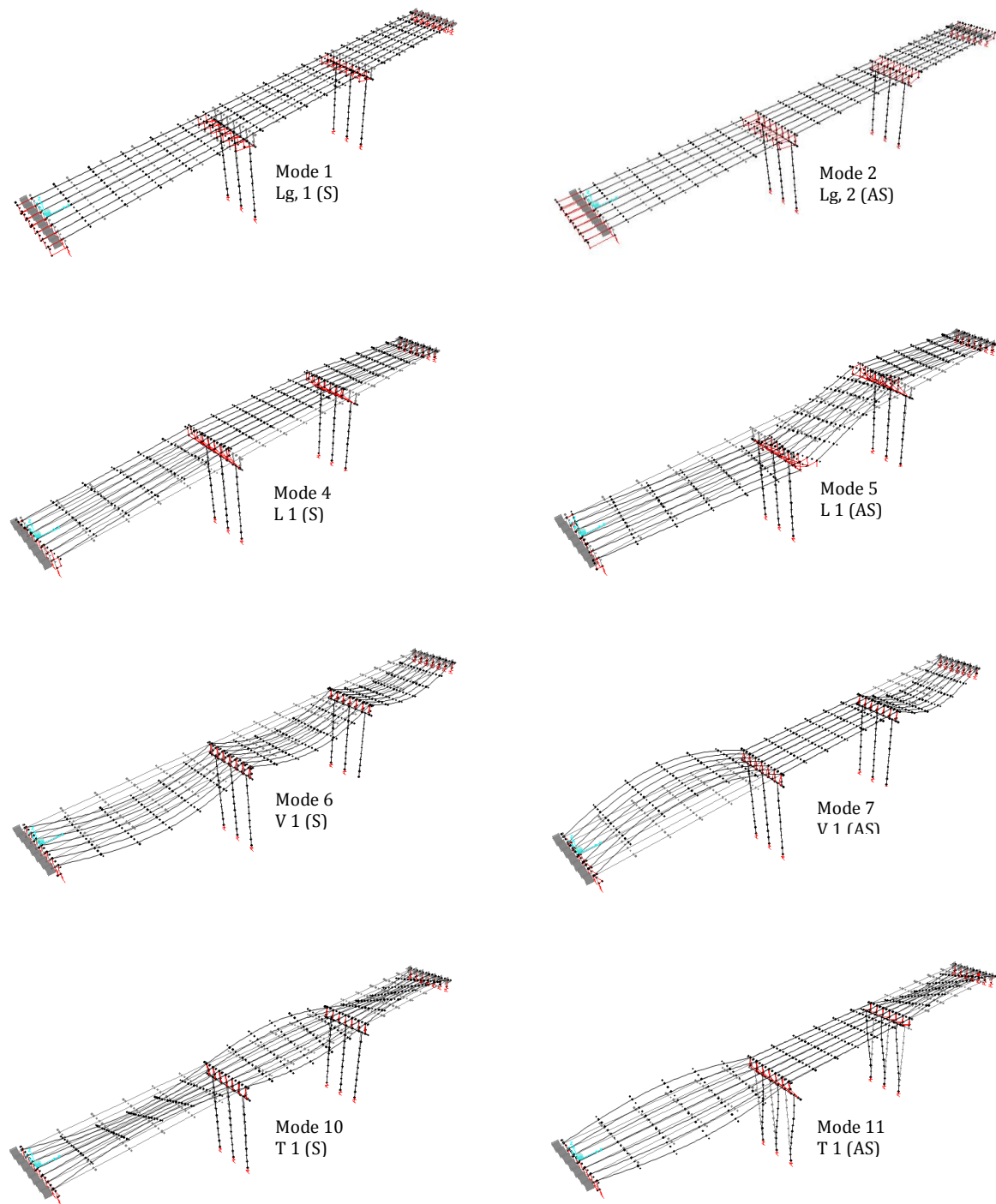


Fig 4. 3-D graphical representation of the mode shapes of both symmetrical (S) and unsymmetrical (AS) fundamental modes of vibration of the MSSS bridge

4. Dynamic analysis of a MSSS prestressed concrete bridge- foundation soil system

In the second part of this study, the previous work is now extended to assess the dynamic analysis of a MSSS prestressed concrete bridge with restrainers and seismic isolation devices including

foundation soil flexibility subjected to a stochastically simulated earthquake based on the design spectrum for the soil type S_2 (firm site) in accordance with RPOA(2008).

Figure 5 show the simulated ground motion compatible with a design spectrum RPOA(2008) scaled by a factor of 2 (i.e. PGA = 0.55g).

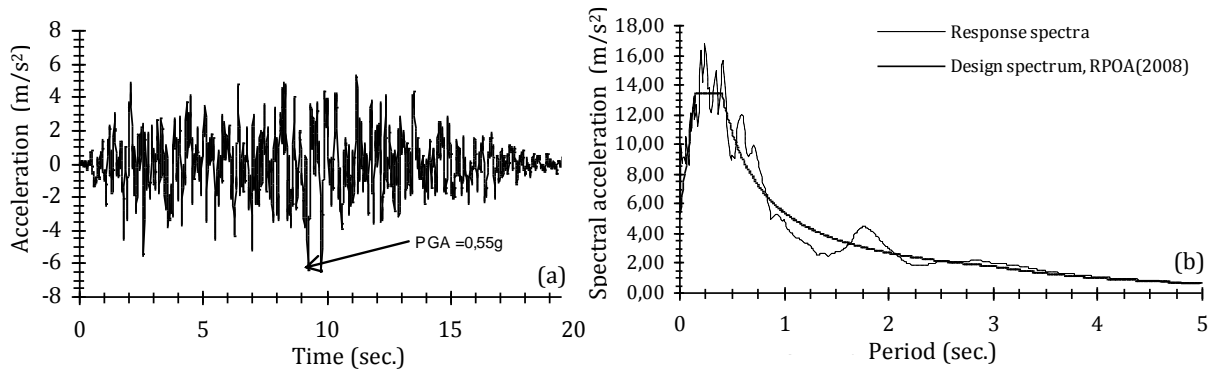


Fig 5. (a) Simulated ground motion, (b) Response spectra and design spectrum RPOA(2008) of the simulated ground motion

For time history analysis of the study bridge response, the mass and stiffness proportional Rayleigh damping coefficients were determined considering the first two modal periods assuming a 5% viscous damping ratio.

The dynamic equations of motion are solved numerically using Newmark’s numerical method (Zienkiewicz and Taylor, 2005; Newmark, 1962).

4.1. Effect of pounding on the gap relative displacement

The absolute maximum gap relative displacements of expansion joints at abutments and at intermediate bents of the MSSS bridge with and without completely elastic pounding are determined in the longitudinal direction (i.e. in the most critical direction). The results obtained are reported in Table 5.

Table 5. Effect of pounding on the absolute maximum gap relative displacements (m) of the girders.

Locations	Abutment expansion joints			Multi-column bents		
	Corner	Intermediary	Central	Corner	Intermediary	Central
Without pounding	0.2054	0.2036	0.2000	0,0301	0,0252	0,0175
With pounding	0,1108	0,1029	0,1015	0,0389	0,0347	0,02553

From Table 5 it is clear that the absolute maximum gap relative displacement is larger at abutment expansion joints, especially in the corner girder. By comparing the pounding effects, we can also see that the absolute maximum gap relative displacements are reduced at abutments and amplified at bents when the pounding effects are considered.

For illustration purposes, the time history responses of bridge in term of relative displacements without and with pounding are depicted in Figures 6(a) for expansion joints of abutments and in 6(b) for expansion joints of intermediary multi-column bents of the study bridge.

It observed that the pounding effects generally lead to a decrease in gap relative displacements at the joint expansions of abutments (see Figure 6(a)) and an increase at the expansion joints of bents (see Figure 6(b)).

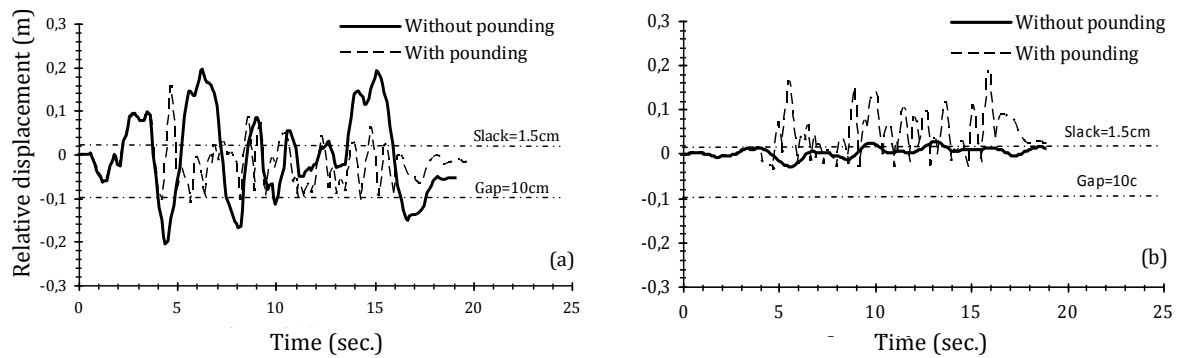


Fig 6. Time history response of absolute maximum relative displacement; (a) Expansion joints of abutments, (b) Expansion joints of intermediate multi-column bents

4.2. Effect of pounding on the peak LRB shear strain

The maximum shear strains in the longitudinal direction of lead rubber bearings LRB located at abutments and multi-column bents of the MSSS bridge with and without pounding are given in Table 6 below.

Table 6. Effect of pounding on the maximum shear strain of lead rubber bearings (in %)

Locations	Abutment expansion joints			Multi-column bents		
	Corner	Intermediary	Central	Corner	Intermediary	Central
Without pounding	413	409	377	442	440	435
With pounding	244	241	303	245	248	252

It is seen that the maximum values of bearings shear strain located on abutments and multi-columns bent are more pronounced when the pounding effects are neglected.

Moreover and for the purpose of illustration, Figures 7(a) and 7(b) below show the time-history response in the longitudinal direction of LRB seismic isolation devices at abutment back wall and multi-column bents.

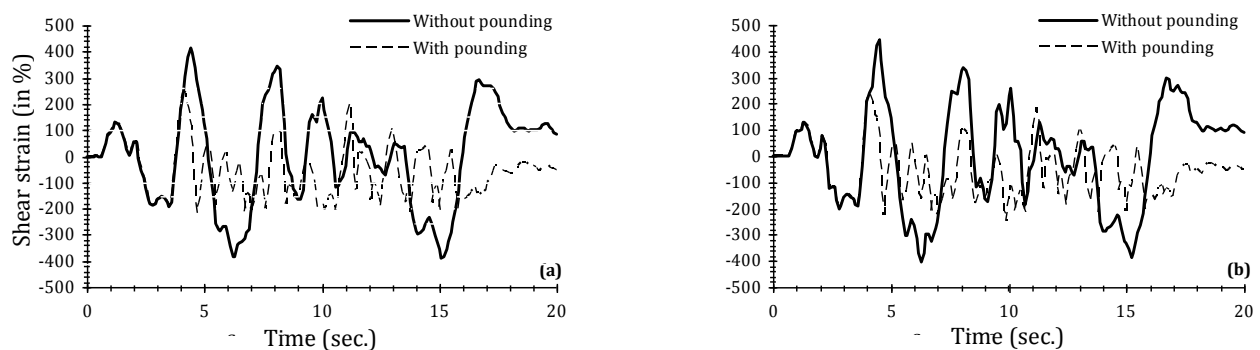


Fig. 7. Time history response of shear strain response of LRB seismic isolation device at abutments (a) multi-columns bent (b) of bridge model.

4.3. Effect of restrainer on the relative displacement of expansion joints

The restrainers used in seismic design of the study bridge are steel cables. The latter are modelled as a multi-linear model with strain hardening and the axial forces are generated when restrainers get engaged by losing the initial slack of 15mm. The yield force of restrainers is 2640 kN/m and initial modulus of elasticity is equal to 69000 MPa. The initial stiffness of the restrainers is 30 kN/mm and a strain hardening of 5% is assumed.

Figure 8 below, depict the temporal variations of relative displacements of expansion joints at abutments and intermediate multi-column bents of the MSSS bridge with and without restrainers.

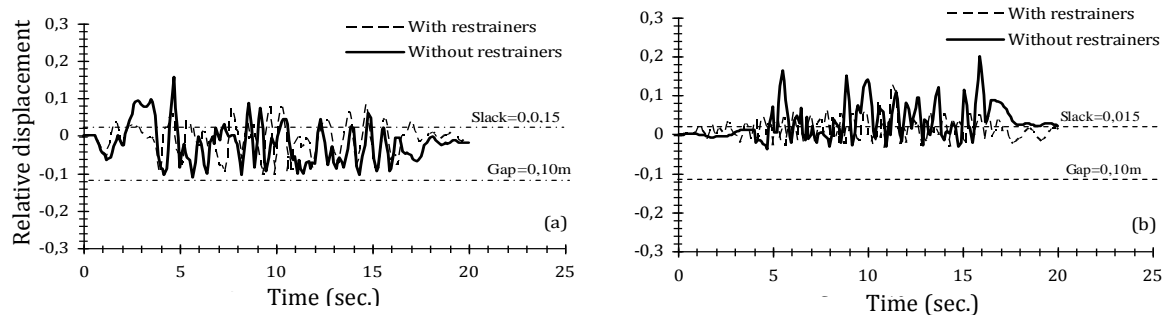


Fig 8. Time history response of absolute maximum relative displacement; (a) Expansion joints of abutments, (b) Expansion joints of intermediary multi-column bents

From Figure 8(a) it is seen that the values of relative displacements of expansion joints of abutments are reduced (indicated by the dash-dotted line) when using the restrainers combined with pounding elements and seismic isolation bearings. Similar trends are observed in the expansion joints of intermediary multi-column bents (see Figure 8(b)).

We can summarize that the restrainers could control the expansion joint opening deformation and secure the unseating of the bridge deck on the expense of the increase of shear and moment seismic demand of the supporting pier at the expansion joint.

4.4. Effect of restrainer on the shear strain response of LRB seismic isolation device

In order to understand the influence of restrainer cables on the LRB seismic isolation device response in the longitudinal direction for study bridge under simulated earthquake, shear strains time variations for these isolators at abutments and bents are plotted in Figure 9.

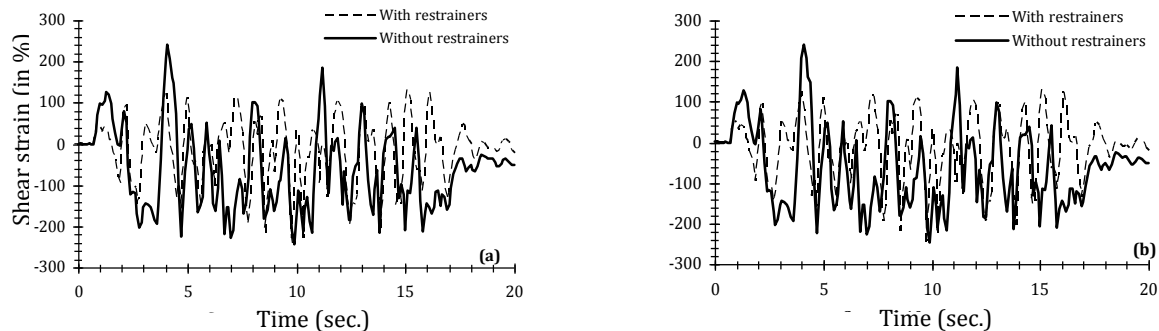


Fig 9. Time history response of shear strain response of LRB seismic isolation device of bridge model (a) at abutments (b) at multi-columns bent.

From Figure 9(a) it is observed that, there is a significant reduction of LRB isolators shear strains at abutments due to the application of restrainer cable system. The bearing peak shear strain at abutment locations is found to be 240% for bridge without the restrainer cables, while it is equal to 132% for bridge with restrainer cables which corresponds to significant decreases of 45% when the restrainer cables system is considered. Similar conclusions can be drawn for LRB isolators shear strains at multi-columns bents Figure 9(b).

Therefore, the restrainer cables tend to reduce the earthquake forces induced in the seismic isolation system of a multi-span simply supported bridge. Under extreme seismic excitations, the maximum bearing shear strain is a quantity of prime interest in the seismic design of bridge structures because if it exceeds certain limits, the bearings may fail resulting into the bridge collapse.

4.5. Effect of restrainers on pounding forces

The gap element is provided to take care of pounding effects between the abutment-deck and deck-deck. The initial gap provided in the gap element is 0.10 m and pounding develops the compressive forces at the interfaces when the relative displacement exhausts this initial gap width. It is modeled by introducing a linear spring with stiffness $K_{Gap} = 3790622$ KN/m at abutments and equal to 1895511 KN/m at bents.

To investigate the effect of restrainer cables on the pounding response at deck-abutment and deck-deck interfaces of MSSS bridge, the temporal variations of the pounding forces without and with restrainers are presented in Figure 10.

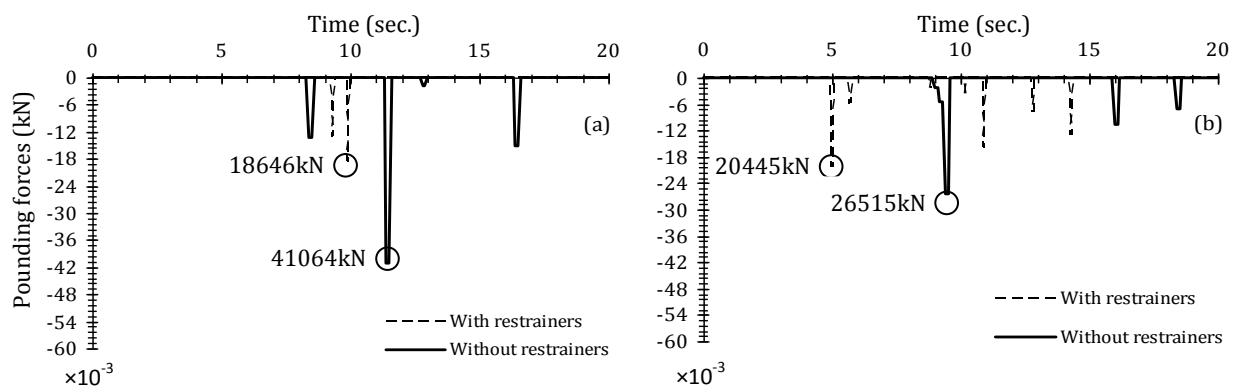


Fig 10. Time history response of pounding forces of bridge model(a) at abutments (b) at multi-columns bents.

From Figure 10 (a), it can be noticed that the restrainer cables reduce significantly the values of pounding forces at the interface of abutment-deck of study MSSS bridge. The maximum pounding force is found to be 41064kN for bridge without restrainers, while it is equal 18646kN when the bridge spans are connected with restrainer cables system. Similar conclusions can be drawn for pounding forces at multi-columns bents (see Figure 10(b)). From the same Figure, it is seen that, there is a substantial 23% reduction in the peak pounding forces at multi-columns bents due to restrainer cables effects.

It can be concluded that the maximum pounding force at expansion joints of a multi-span simply supported MSSS concrete bridge is obviously reduced using restrainer cables system.

5. Summary and Conclusions

In this paper, an extensive numerical investigation on the dynamic analysis of a multi-span simply supported MSSS prestressed concrete bridge with expansion joints and lead rubber bearing devices including foundation soil flexibility effects are presented. In this context, the 3D Finite Element Model FEM of a MSSS bridge subjected to a 3D components of severe seismic excitation is performed in order to assess the performance of steel restrainer cables and Lead Rubber Bearing devices LRB. The Nonlinear hysteretic models characterizing the seismic behavior of various bridge components (including expansion joints and bearing devices) are considered.

The effects of restrainer cables and pounding forces on the MSSS bridge behavior are discussed, and the following conclusions are drawn:

1. The first three dominant modes of the bridge are in the longitudinal directions which to assess a dynamic analysis in this direction (i.e. in the most critical direction).
2. Pounding effects generally lead to a decrease in gap relative displacements at abutment joint expansions and increase at bent expansion joints.

3. The computed maximal shear strains of LRB in the longitudinal direction are more pronounced when the pounding effects are neglected.

A comparative assessment of behaviour of expansion joints, lead rubber bearing devices and steel restrainers components shows that under this study:

- i. The restrainers could control the expansion joint opening deformation and secure the unseating of the bridge.
- ii. The steel restrainer cables tend to reduce the earthquake forces induced in the seismic isolation devices LRB of a multi-span simply supported bridge.
- iii. Under extreme seismic excitations, the peak shear strain at bearing devices is a quantity of prime interest in the design of bridge structures because if it exceeds certain limits, the bearings may fail resulting into the bridge collapse.
- iv. The maximum pounding forces at expansion joints of a multi-span simply supported MSSS concrete bridge are obviously reduced using restrainer cables system.

It follows that in order to ensure an acceptably safe structural performance of a MSSS prestressed concrete bridge with expansion joints and seismic isolation system LRB at abutments, due consideration should be given at design stage to:

- Sound evaluation of distortion limits of seismic isolation bearings LRB at expansion joints and the restrainers components capacities at expansion joints.
- Using restrainers combined with the seismic isolation systems at bridge expansion joints could be an effective method of reducing the large pounding forces and preventing unseating damage.

6. References

- Anagnostopoulos, SA. & Spiliopoulos, KV. (1992) An investigation of earthquake induced pounding between adjacent buildings. *Earthquake eng. struct dyn.*, 21, 289–302.
- Association Francaise de Génie Parasismique AFPS (2003). Séisme de Boumerdes du 21 Mai 2003: Rapport préliminaire de la mission AFPS Organisée avec le concours du Ministère de l'Habitat.
- Bi, K.M., Hao, H. & Chouw, N. (2013). 3D FEM analysis of pounding response of bridge structures at a canyon site to spatially varying ground motions. *Advances in Structural Engineering*, 16 (4), 619-640.
- Chopra, A. K. (2011). *Dynamics of structures: Theory and applications to earthquake engineering*. Prentice-Hall, New Jersey, USA.
- Chouw, N. (1995). Effect of the earthquake on 17th of January 1995 on Kobe. In *Proceedings of the D-A-CH Meeting of the German, Austrian and Swiss Society for Earthquake Engineering and Structural Dynamics*, University of Graz, Austria, pp. 135- 169.
- CSI Bridge 2015 V 17.2.0 . Computer and Structures Inc. SAP2000 (Nonlinear Version 15), Nonlinear user's Manual Reference. USA.
- Desroches, R. & Delemont, R. (2002). Seismic retrofit of simply supported bridges using shape memory alloys. *Engineering structures*, 24, 325–332.
- Desroches, R. & Muthukumar, S. (2004) Implications of seismic pounding on the longitudinal response of multi-span bridges—an analytical perspective. *Earthquake engineering and engineering vibration*, 3, 57–65.
- FEMA 273 NEHRP (1997). *Guidelines for the Seismic Rehabilitation of Buildings*, Federal Emergency Management Agency. Washington D.C, USA.
- FEMA-356 (2000). *Prestandard and commentary for seismic rehabilitation of buildings*, Federal Emergency Management agency, Washington, DC, USA.

- Gazetas, G. (1991). Foundation Vibrations: chapter 15, In *Foundation Engineering Handbook*, H-Y Fang H-Y, Van Nostrand Reinhold, New York.
- Hong, Y.J., Xian, L.L., Nan L., Jian, Y., Shi-Xiong, Z. & Chao, Z. (2019). Nonlinear pounding analysis of multi-span and simply supported beam bridges subjected to strong ground motion. *Shock and vibration*, 1-11.
- Hung, C. J. Lin, H., Liu, Y. & Chai, J. (2008, October). Reconnaissance report of 0512 China Wenchuan earthquake on bridges. In *Proceedings of the 14th World Conference on Earthquake Engineering*, Beijing, China.
- Kawashima, K. & Shoji, G. (2000, February). Effect of restrainers to mitigate pounding between adjacent decks subjected to a strong ground motion. *Proceedings of 12th world conference on earthquake engineering*, Auckland, New Zealand.
- Newmark, N. M. (1962). A Method of computation for structural dynamics," *Trans. ASCE*, 127.
- Ouanani, M. & Tiliouine, B. (2015). Effects of foundation soil stiffness on the 3-D modal characteristics and seismic response of a highway bridge. *Journal of Civil Engineering KSCE*, 19(4), 1009-1023.
- Ouanani, M. & Tiliouine, B. (2017). Progressive seismic failure of a highway bridge, including abutment-backfill interaction. *Current science*, 112(2), 355-363.
- RPOA (2008). Règles Parasismiques Applicables au Domaine des Ouvrages d'Art. Document Technique Règlementaire, Ministère des Travaux Publics, Alger, Algeria.
- Schnabel, P. B., Lysmer, J. & Seed, H.B. (1976). A Computer Program for Earthquake Response Analysis of Horizontally Layered Sites (SHAKE), Report (EERC 72 12), Earthquake engineering research center, University of California, Berk'eley.
- Shinozuka, M., Murachi, Y., Dong, X., Zhou, Y. & Orlikowski, M. (2003) Effect of seismic retrofit of bridges on transportation networks. *Earthquake engineering and engineering vibration* , 2, 69-179.
- Tazarv, M. & Alam, S. (2018, June). Shape memory alloy for bridge columns. *Proceedings of the eleventh U.S. National conference on earthquake engineering*, CA, USA.
- Tiliouine, B. & Ouanani, M. (2012, September). 3-D nonlinear earthquake response of R.C. box girder bridges with expansion joints and bearing devices. *15th world conference on earthquake engineering*, Lisbon, Portugal.
- Todd, D., Carino, N., Riley, M., Chung, H. S., Andrew, W., William, D., James, D., and Roland, N. (1994). *The Northridge, California, Earthquake of January 1994: Performance of Structures, Lifelines, and Fire Protection Systems*. National Institute of Standards and Technology (NIST), USA.
- Uzarski, j. & Arnold, C. (2001). Chi-chi, Taiwan, earthquake of September 21, 1999: reconnaissance report. *Earthquake spectra*, supplement, Taiwan.
- Wilson, E. L. (2002). *Three-dimensional static and dynamic analysis of structures: a physical approach with emphasis on earthquake engineering*. Computer and Structure, Inc. Berkeley, California, USA.
- Wolf, J.P. (1997). Springs-Dashpots-Mass models for foundation vibration. *Earthquake engineering and structural dynamics*, 26, 931-949.
- Xu Chena, B. & Chunxiang, Lib. (2020) Seismic performance of tall pier bridges retrofitted with lead rubber bearings and rocking foundation. *Engineering structures*, 212, 1-15.
- Yang, Z., Kun, C & Chouw, N. (2018, December). Impact of spatial variation of ground motions on the seismic performance of a bridge structure. *25th Australasian Conference on Mechanics of Structures and Materials (ACMSM25)*, Australia.
- Yohchia, C. (1996). Modeling and analysis methods of bridges and their effects on seismic responses: I Theory. *Computers and structures*, 59(1), 81-89.
- Zienkiewicz, O.C. & Taylor, R.L. (2005). *The Finite element method, solid mechanics*. Upper Saddle River, New Jersey, USA.
-

© 2020. This work is published under <http://creativecommons.org/licenses/by/4.0/> (the “License”). Notwithstanding the ProQuest Terms and Conditions, you may use this content in accordance with the terms of the License.